

Results of Electromagnetic and Electrical Measurements in Antarctica

B.B. Bhattacharya, M. Keramat* and R.S. Raju

Department of Applied Geophysics, Indian School of Mines, Dhanbad-826004.

ABSTRACT

Transient electromagnetic (TEM) soundings were carried out in Dronning Maud Land region of Antarctica. Self-potential (SP) and vertical electrical sounding (VES) measurements were also made in the Schirmacher Oasis. The thickness of the ice shelf in the Dronning Maud Land is about 200 m. The thickness of the ice cap over the rocky terrain south of Schirmacher Oasis increases rapidly and at the place of TEM sounding is of the order of 400 m. Self-potential profiles do not show any characteristic anomaly. VES data reveal that the depth to fresh rock in the oasis is less than ten metres. There is extensive scope of using TEM method in Antarctica for determining the thickness of ice cover.

INTRODUCTION

Geophysical surveys consisting of transient electromagnetic (TEM), self-potential (SP) and vertical electrical soundings (VES) were carried out in Schirmacher Oasis ($77^{\circ}44'30''$ - $70^{\circ}46'30''$ S; $11^{\circ}22'04''$ - $11^{\circ}54'00''$ E) and in the shelf ice areas near the Indian station of Dakshin Gangotri ($70^{\circ}05'37''$ S; $12^{\circ}00'00''$ E) in Antarctica. The aim of the work was to determine the feasibility of the methods in the Antarctic conditions, and, if possible, to obtain:

- (a) the thickness of the shelf ice in the neighbourhood of Dakshin Gangotri Station,
- (b) the thickness of the weathered zone in the Schirmacher Oasis, and
- (c) self-potential anomaly zone, if any, in the Schirmacher Oasis.

The measurements were carried out in the (summer) months of January and February, 1985 in clear weather on relatively warmer days using transient electromagnetic system of MPPO type designed at ISM (Bhattacharya and Raju, 1986; Raju et al., 1987) and a standard resistivity meter respectively. These types of geophysical measurements, as far as is known, have not been carried out by the Indian, Soviet or other countries in these areas till 1985.

INSTRUMENTS

Self-potential and VES measurements were carried out by standard resistivity meters and the details of the equipment are well known. The essential features of the TEM system are given below.

The general field layout for the TEM method with MPPO system is shown in Fig. 1. The basic principle of the transient measurement is shown in Fig. 2. The measurements are made during the switch off period. The block diagram of the system is given in Fig. 3. The instrument consists of a transmitter and a receiver both housed in a single box.

*Deptt. of Applied Physics and Electronics, Rajshahi University, Rajshahi, Bangladesh. At present with the Deptt. of Applied Geophysics, Indian School of Mines, Dhanbad-826004.

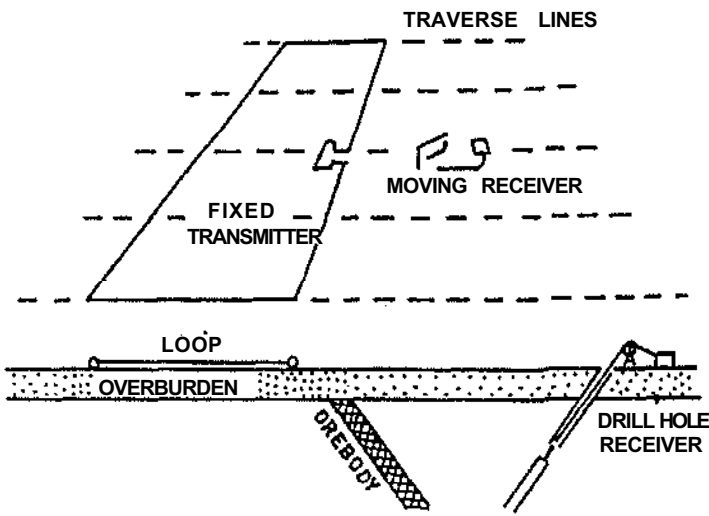


Fig. 1. General field layout for transient electromagnetic (TEM) method including MPPO system.

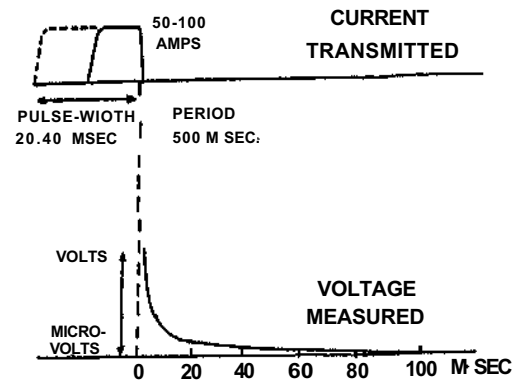


Fig. 2. Transient measurement principle.

BLOCK DIAGRAM, ISMTEM

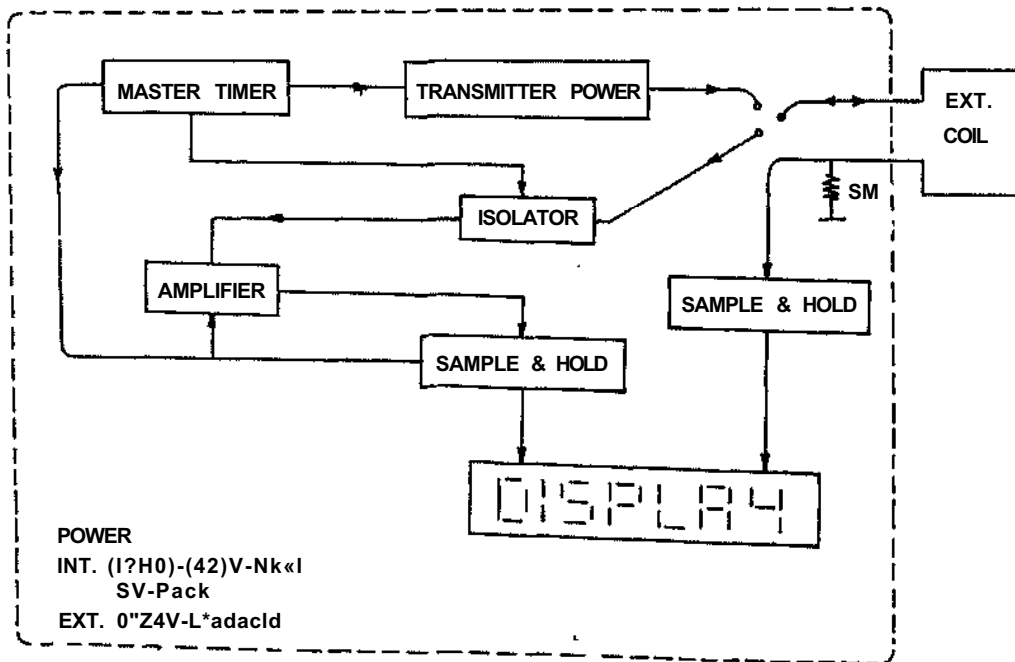


Fig. 3. Block diagram of MPPO transient electromagnetic (ISM TEM) unit.

The transmitter consists of a pulse generating circuit providing 20 ms "ON" and 30 ms "OFF", i.e., with 40% of the duty cycle. The fall time of the transmitter current is 10 μ s. The maximum pulse current is 10 amp. In the TEM method, a rectangular or square loop is placed over the surface and a rectangular pulsed current is momentarily sent through the loop. The secondary field induced by the eddy current is measured after the switch off. The signal received during the off time is amplified and processed. This is transient in nature which is sampled at various preselected time intervals which in turn is displayed in the display unit.

The coil consists of bare enamelled copper wire of 18 SWG. The criteria for the selection of gauge depends on easy handling of the wire in the field and the maximum current to be sent. Thus a compromise has to be made between the thickness and the resistance of the coil. The size of the loop in the field can be 500 m X 500 m; 200m X 200m; 100m X 100m; 50m X 50m; 10m X 10m. The loop size is decided by the user depending on the nature of the problem.

Isolator is an important block in the design of TEM unit. It is achieved in the unit by the use of fast acting reed relays and an analog switch. This block acts as a separator between the transmitter and receiver with the coil. Amplifier is the heart of the system. The FET input amplifier is used as it provides a high input impedance. A total gain change of 0 to 80 db is provided in steps of 20 db variation. This takes care of signal measurements from 1 to 9 channels as required for the wide range of signal. The signal response is limited to 10 kHz.

The output of the amplifier is sampled at 1, 2, 3, 4, 5, 6, 7, 8, 9 ms as determined by the switch positions after the switching off of the transmitter current. The sampled output is then held by the IC sample and holder. Another sample is taken after 20 ms after the switch off which provides the background noise level. The difference of the earlier sample and this provides the actual signal, provided that the signal decays before 20 ms. The difference signal is then held by another sample holder for the continuous display.

The signal processed are then converted from its analog form to digital. A 3.1/2 digital display is used to display the signal voltages. External battery, either lead acid or Ni-Cd, can be used for the transmitter current.

MATHEMATICAL DEVELOPMENT OF TEM PROBLEM FOR THE STUDY OF THICKNESS OF ICE SHELF

Transient responses due to a finite horizontal loop excited by a rectangular current pulse have been developed. To obtain complete generality in the solution, the final expression is obtained numerically. We have considered the cylindrical symmetry of the problem to get the scalar electric field component. Let us consider a horizontal circular loop of radius b located at a height h above a uniform ground. The origin of the coordinate system is considered at the centre of the coil with the Z-axis coinciding the axis of the coil as shown in Fig. 4.

The expression of the secondary electric field at a distance r due to the ground is given by Morrison et al. (1969):

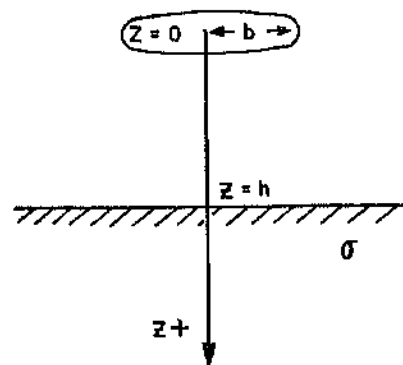


Fig. 4. Loop geometry.

$$E(t) = \frac{j\mu w b I}{2} \int_0^{\infty} J_1(\lambda b) J_1(\lambda r) \frac{n_1 - \lambda}{n_1 + \lambda} \cdot e^{-2\lambda h} d\lambda \quad \dots(1)$$

where, I is the current in the loop, $n_1 = \sqrt{\lambda^2 + j\omega\mu}$

The emf induced in the loop is then,

$$E = 2\pi b \cdot E(b)$$

$$i.e., E = j\omega\mu\pi b I \int_0^{\infty} J_1^2(\lambda b) \frac{n_1 - \lambda}{n_1 + \lambda} \exp(-2\lambda h) d\lambda \quad \dots(2)$$

The expression can be simplified by writing $x = \lambda b$, thus

$$E(j\omega) = j\omega\mu\pi b I (j\omega) \int_0^{\infty} J_1^2(x) \left\{ 1 - \frac{2x}{m_1 + x} \right\} \exp(-2gx) dx \quad \dots(3)$$

It is the steady-state secondary electric field induced in the loop. The time domain response $e'(t)$ can be obtained from the equation (3) by writing $s = j\omega$ and then taking the inverse Laplace transform of that function. The emf due to the pulse current wave form is then

$$E(s) = \pi \mu b I_0 \int_0^{\infty} J_1^2(x) [1 - \exp(-st_0)] \left\{ 1 - \frac{2x}{m_1 + x} \right\} \exp(-2gx) dx \quad \dots(4)$$

where, I_0 is the current amplitude, $g = h/b$ and $m_1 = (x^2 + S\mu\sigma b^2)^{1/2}$

Now taking the inverse Laplace transform of equation (4) and for time $t > t_0$, we have

$$e(t) = 2\sqrt{\pi\mu b I_0} \int_0^{\infty} \left[\frac{1}{t} \cdot \sqrt{\frac{\mu b^2 \sigma}{t}} \cdot J_1^2 \left(Y \sqrt{\frac{\mu b^2 \sigma}{t}} \right) \cdot \exp \left(-2g \sqrt{\frac{\mu b^2 \sigma}{t}} \cdot Y \right) \cdot Y \{ Y \sqrt{\pi} \operatorname{erf}(Y) - \exp(-Y^2) \} dY + \frac{1}{t-t_0} \cdot \sqrt{\frac{\mu \sigma b^2}{t-t_0}} \cdot J_1^2 \left(Y_1 \sqrt{\frac{\mu \sigma b^2}{t-t_0}} \right) \cdot \exp \left(-2g \sqrt{\frac{\mu \sigma b^2}{t-t_0}} \cdot Y_1 \right) \cdot Y_1 \{ Y_1 \sqrt{\pi} \operatorname{erf}(Y_1) + \exp(-Y_1^2) \} dY_1 \right] \quad \dots (5)$$

where, $Y = x \sqrt{\frac{t}{\mu \sigma b^2}}$ and $Y_1 = x \sqrt{\frac{t-t_0}{\mu \sigma b^2}}$

Now with the help of Neumann's series and exponential function series representation, we can simplify the equation (5). Using the transform pair numbers (3.46) and (6.28) in Gradshteyn and Ryzhik (1965, p. 337 and p. 648), we get finally,

$$\frac{e(t)}{I_0} = \sqrt{\pi} \mu b \sum_{m,k=0}^{\infty} \frac{(-1)^{m+k} \cdot (2m+2)!}{m! k! (m+2)! [(m+1)!]^2} \cdot \left(\frac{2m+k+2}{2} \right)!$$

$$\frac{1}{2m+k+5} \cdot \frac{1}{2^{2m-k+2}} \cdot \left(\frac{h}{b}\right)^k \cdot \left[\frac{1}{t-t_0} \left(\frac{\mu\sigma b^2}{t-t_0}\right)^{\frac{1}{2}(2m+k+3)} - \frac{1}{t} \cdot \left(\frac{\mu\sigma b^2}{t}\right)^{\frac{1}{2}(2m+k+3)} \right] \quad \dots(6)$$

For a square loop of L X L size instead of the circular loop of radius *b* and neglecting the higher order terms, the equation (6) becomes,

$$\frac{e(t)}{I_0} = \mu L \left[\frac{1}{t-t_0} \cdot \left(\frac{\mu\sigma L^2}{\pi(t-t_0)}\right)^{3/2} \cdot \left\{ 1/20 - \frac{\pi}{16} \cdot \frac{h}{L} \cdot \sqrt{\frac{\mu\sigma L^2}{\pi(t-t_0)}} \right\} - \frac{1}{t} \cdot \left(\frac{\mu\sigma L^2}{\pi t}\right)^{3/2} \cdot \left\{ 1/20 - \frac{\pi}{16} \cdot \frac{h}{L} \cdot \sqrt{\frac{\mu\sigma L^2}{\pi t}} \right\} \right] \quad \dots(7)$$

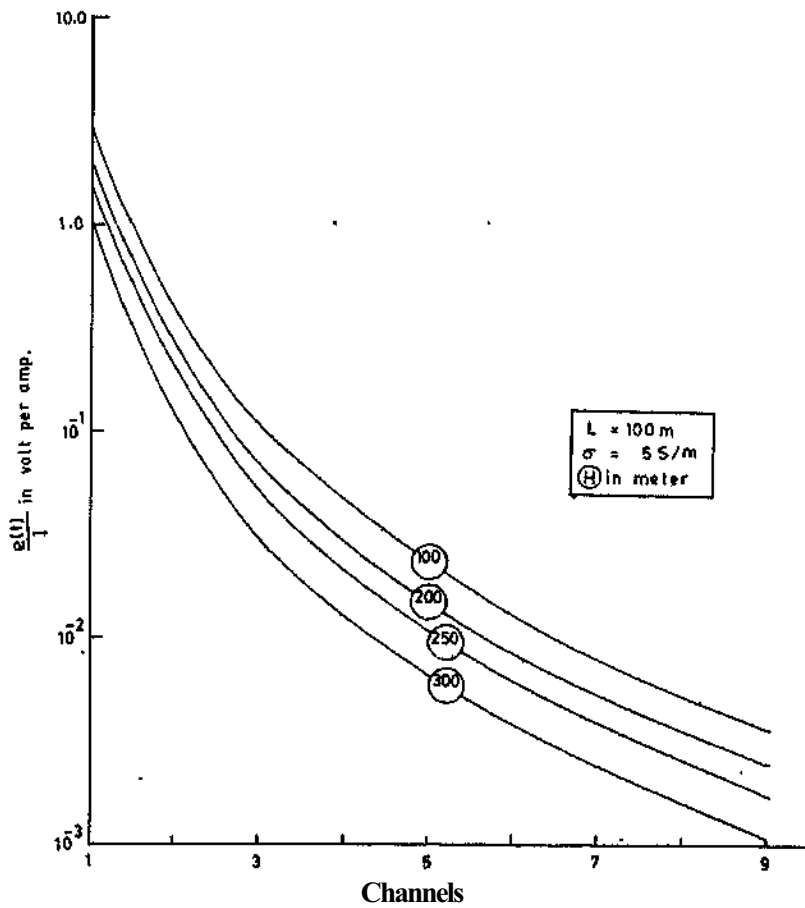


Fig. 5. Theoretical TEM response curve.

An album of the response curves for the different loop sizes, heights of the loops and conductivities of the half-space can be prepared from the equation (7). One curve from the album is reproduced here (Fig. 5). The observed field transient curve can be matched with the curves of the album and the parameters of the theoretical curve giving the best fit to the field curve may be considered as the parameters of the field giving rise to the observed transient response.

Nomogram and conductivity aperture diagrams have been prepared, using the equation(7), for the determination of the thickness of the insulating overburden (H) and conductivity of the half-space (σ) using the responses $[e(t)/I]$ at different channels. Fig. 6 shows the nomogram for the channels 3 and 6 for the different overburden thicknesses (H = 100, 200, 300m) and the conductivities of half-space ($\sigma = 5, 10$ S/m). Thus using this nomogram, one can obtain the approximate value of the height of overburden as well as the conductivity of half-space using the responses of the channels 3 and 6 only for a given loop size. Fig. 7 shows the response of the channel 5 for different conductivities and overburden thickness. From the response of the channel 5, one can obtain a relatively closer range of the conductivity. Thus an interpreter, if it is so required, can prepare a theoretical response curve using these parameters for still better matching of the field and theoretical curves.

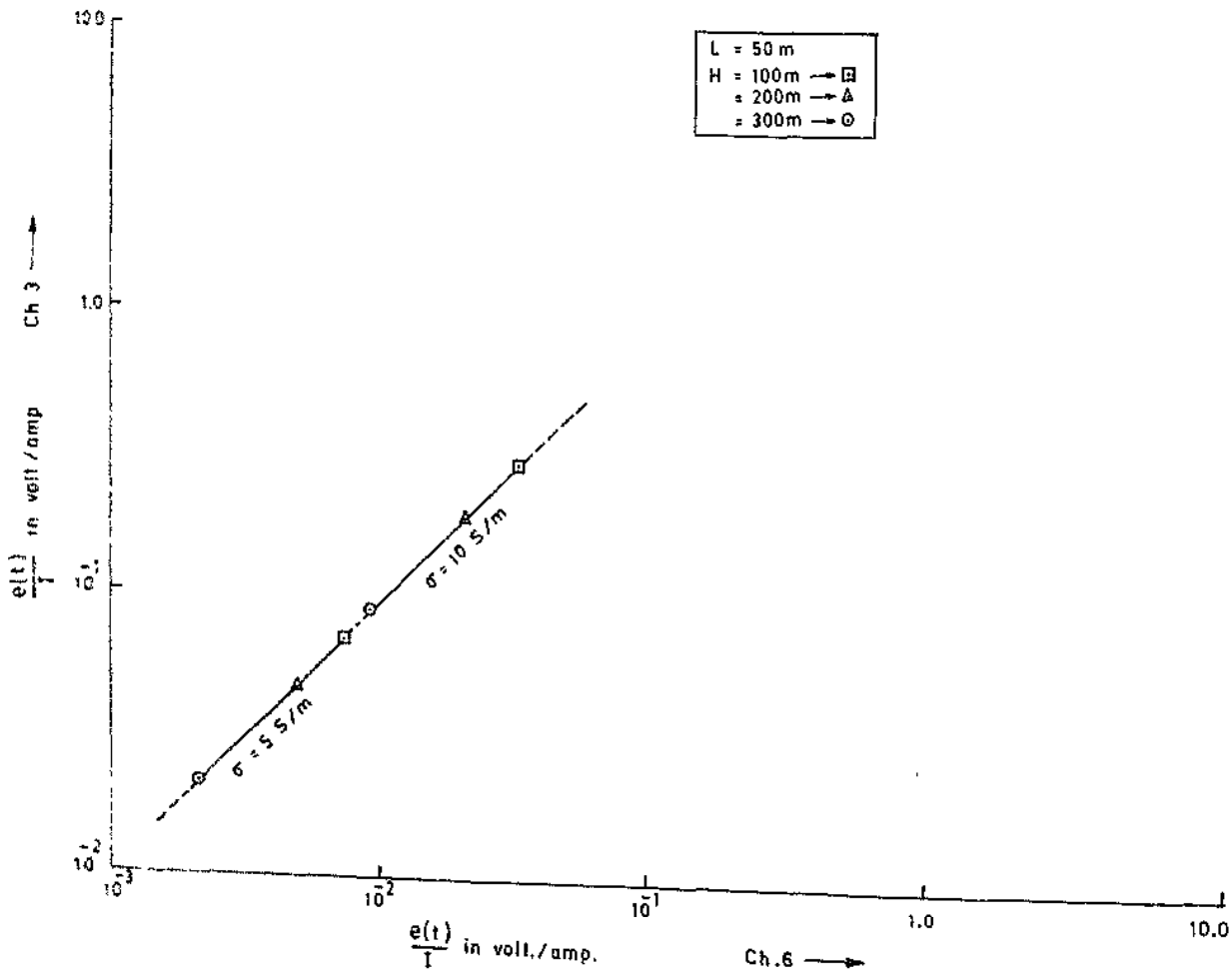


Fig. 6. Nomogram for TEM sounding interpretation.

GEOLOGY

An apron of ice around the Antarctic landmass extends up to 100 km and rises to a height of 100 m. The Indian permanent station, Dakshin Gangotri (70°05'S; 12°00'E) is located in one such ice shelves of Antarctica (Fig. 8). The coastal parts of the shelf do not show any major topographic change. The ice shelf abruptly rises to a height of 50 to 60 m for the first 10 km or so and then gradually slopes downward till the northern face of the Schirmacher Oasis. At this site, two lagoon like features are formed, surrounded on the three sides by the highly controlled shelf ice and on the fourth side by the land mass. These lagoons mark the exposed parts of the sea surface. Thinning of the shelf ice at this region may be due to high radiation caused by the reflection of the sunlight from the rock cliffs (Raina et al., 1985). The shelf ice topography up to 40 km from the coast is undulating in nature with some sastrugis oriented in N80°E-S80°W direction. Beyond this region, a network of

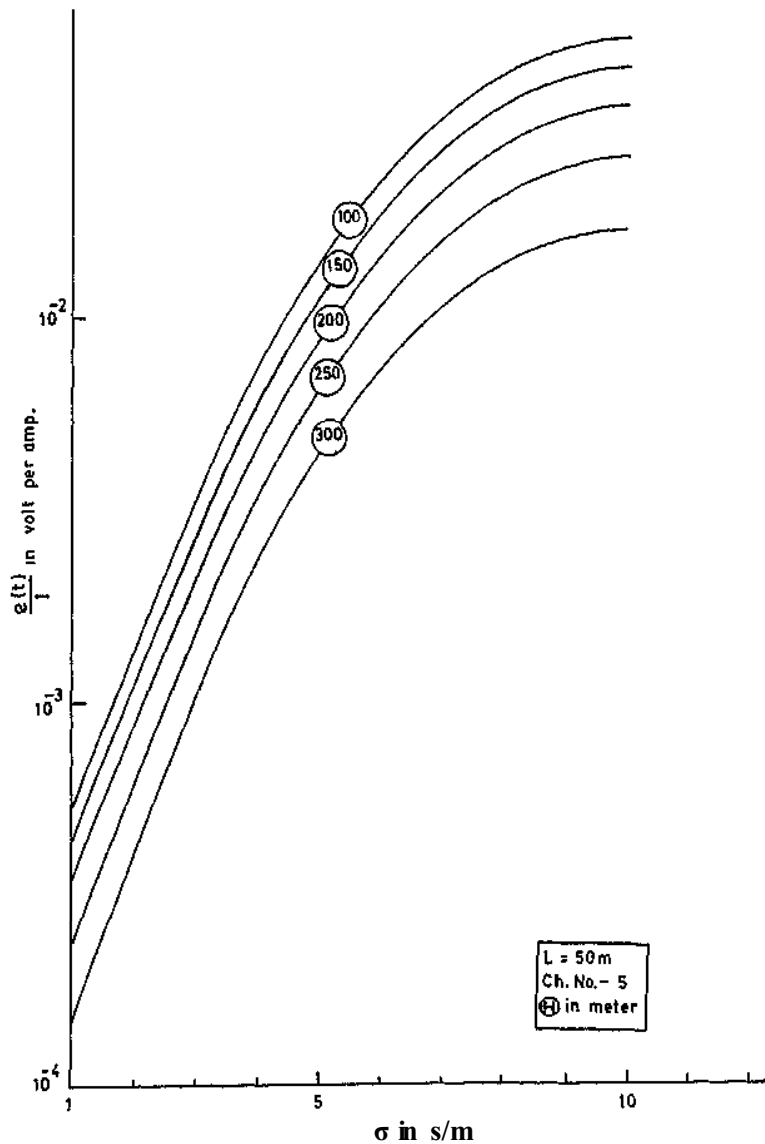


Fig. 7. Conductivity aperture diagrams for TEM system.

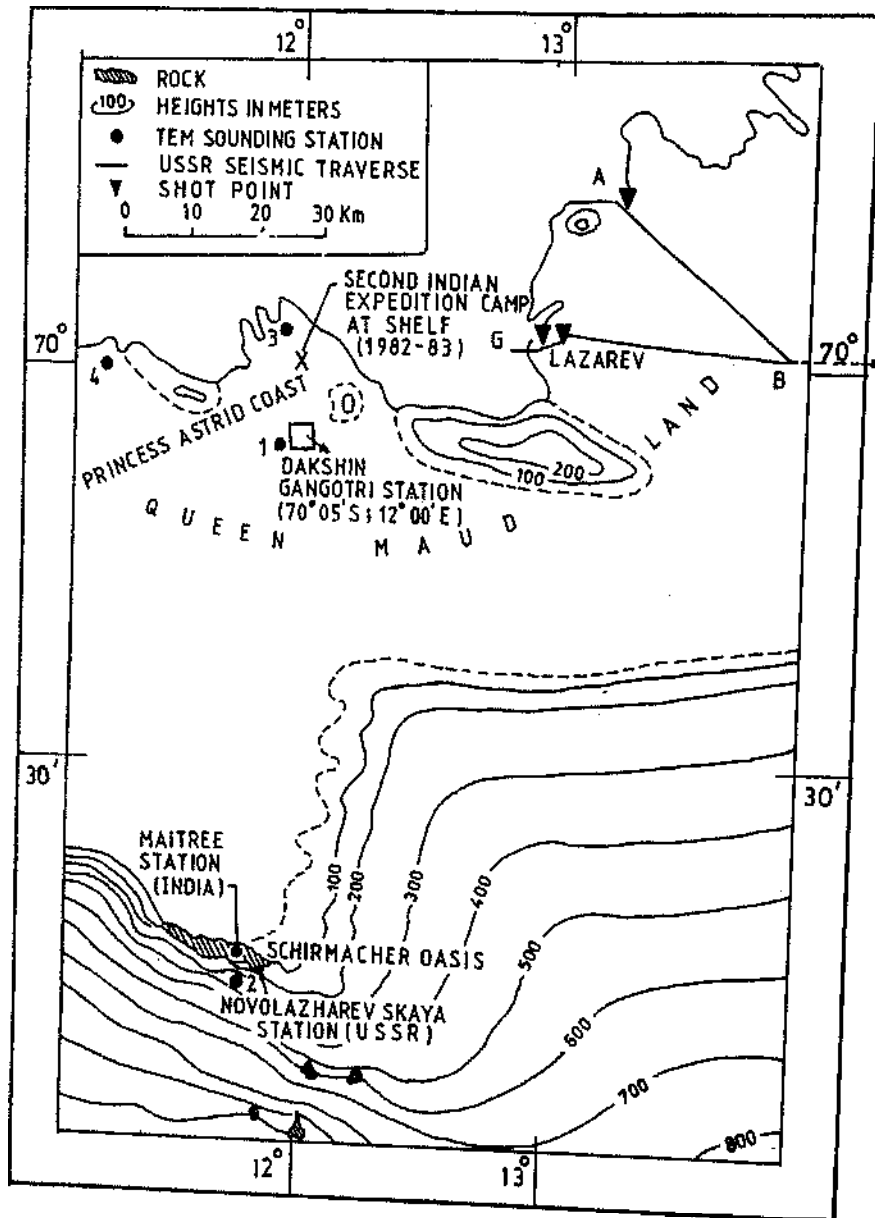


Fig. 8. Location map for geophysical studies.

melt channels covers the ice shelf, and further south the channels turn into a vast lake. The flow of water everywhere is from the east to the west. The density of the shelf ice is of the order of 0.5 gm/cc and the hardness varies from 5 to 10 kg/cm^2 (Raina et al., 1985). The correlation of the ice rise (a number of them seen here) from the satellite imagery and that of the description by Olav (1978) gives a confirmation that no major change in the coastal feature has taken place during the last one decade. These ice rises are possibly the continental shelf rises which have been overridden by the shelf ice and the former now hold the shelf in more or less stable position.

Schirmacher Oasis forms the foothill zone of the mountain ranges of the Queen Maud Land (Fig. 8) and lies almost midway between the Indian Station (Dakshin Gangotri) towards north and

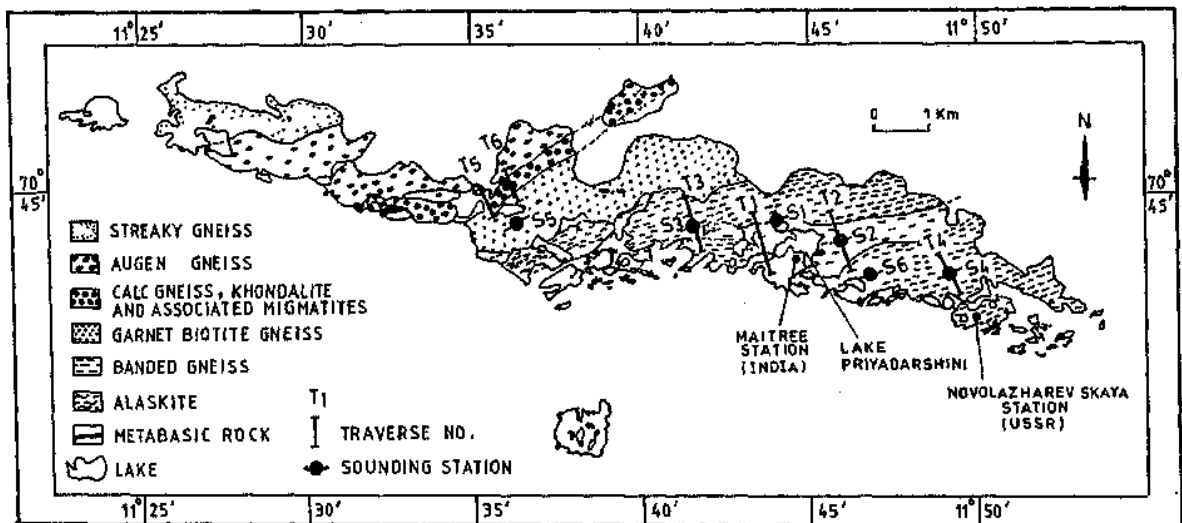


Fig. 9. Geological map showing self-potential traverses and VES locations.

the Wohlthat mountain ranges in the south. The geology of the area is described on the basis of the work carried out by Kaul et al. (1985), Sengupta (1986) and Singh (1986). The Schirmacher Oasis belongs to the East Antarctica Charnokite Province (Fig. 9). The rocks have undergone several stages of metamorphism, migmatization and deformation. The main lithological varieties are: charnockite, granite gneisses, gneissose migmatites of different varieties, relicts of metabasic rocks, calc-silicates and aluminous gneiss. The area can be mapped out into six major lithological units: (a) banded gneiss, (b) alaskite, (c) garnet biotite gneiss, (d) calc-gneiss, khondalite and associated migmatites, (e) augen gneiss and (f) streaky gneiss. The oasis is roughly east-west oriented. The six lithological units have an ENE trend intersecting the hill range at low angle (Fig. 9).

The major portion of the eastern Schirmacher Oasis displays prominent banding with considerable compositional difference. The major units in the banded gneiss are: (1) pyroxene granulite and biotitised pyroxene granulites; (2) brownish-red garnetiferous and pyroxene bearing variety without notable amphibole or biotite; (3) gneisses containing lenses of dark minerals mainly containing pyroxene. The darker varieties grade into pyroxene granulite and are essentially composed of biotite with some amphibolites. Alaskites are light grey or off-white in colour without distinct colour banding and contain variable amounts of garnet. The garnet biotite gneisses are characterised by the presence of large elongate clots of garnet and biotite. A few thin discontinuous bands of biotitised amphibolite run through this gneiss without any regular banded character. The calc-gneiss, khondalites and associated migmatites unit is layered with individual layers varying from a few centimetres to a few metres. The colour banding in the calc-gneiss is partly represented by the variable calc-silicate assemblages in different layers and partly by lit-par-lit emplacement of the granitic material. Banding is accentuated by thin zones of mylonite which alternate with the less sheared rocks. A separate body of pyroxene granulite occurs within the north-eastern part of the band. Although khondalites occur in association with the banded gneisses, alaskite and calc-gneisses are mostly concentrated within this unit. The rock is characterised by light brownish-yellow colour mottled with coarse crystals of garnet with a banding of alternate garnet rich and quartzo-feldspathic bands with visible specks of

graphite. A thick band of augen gneiss runs through the west-central part of the Schirmacher Oasis. The augens are composed mainly of very coarse feldspar. The rock is occasionally garnetiferous. The augen gneiss does not show colour banding and is mostly devoid of enclaves or bands of pyroxene granulite or amphibolite but remnants of charnockitic rocks are found. The streaky gneiss occurs in the western most end of the oasis with a general appearance similar to the garnet-biotite gneiss but distinguished by the absence of garnet. It is much more schistose or well foliated than the garnet-biotite gneiss and shows evidence of much more penetrative shearing. The streaky gneiss contains several large enclaves of pyroxene granulites with gradations contacts and remnants of charnockitic rocks.

Disseminated grains of pyrite, chalcopyrite, galena and some associated sulphide minerals are present in the calc-gneisses and the associated migmatites. Surficial limonitic encrustations, malachite stains and graphite rich bands are noted in various parts.

FIELD WORK AND RESULTS

Six small traverses (Tr 1 to Tr 6) were laid in the oasis (Fig. 9) approximately perpendicular to the geological strike. Three traverses were laid covering the zones of disseminated mineralization (Tr. 1 and 2) and surficial limonitic encrustations (Tr. 4). The station intervals were 25m. Self-potential measurements were carried out over these traverses. All the traverses show relative potential differences with respect to different bases. Six VES soundings (S1 to S6) were also carried to different

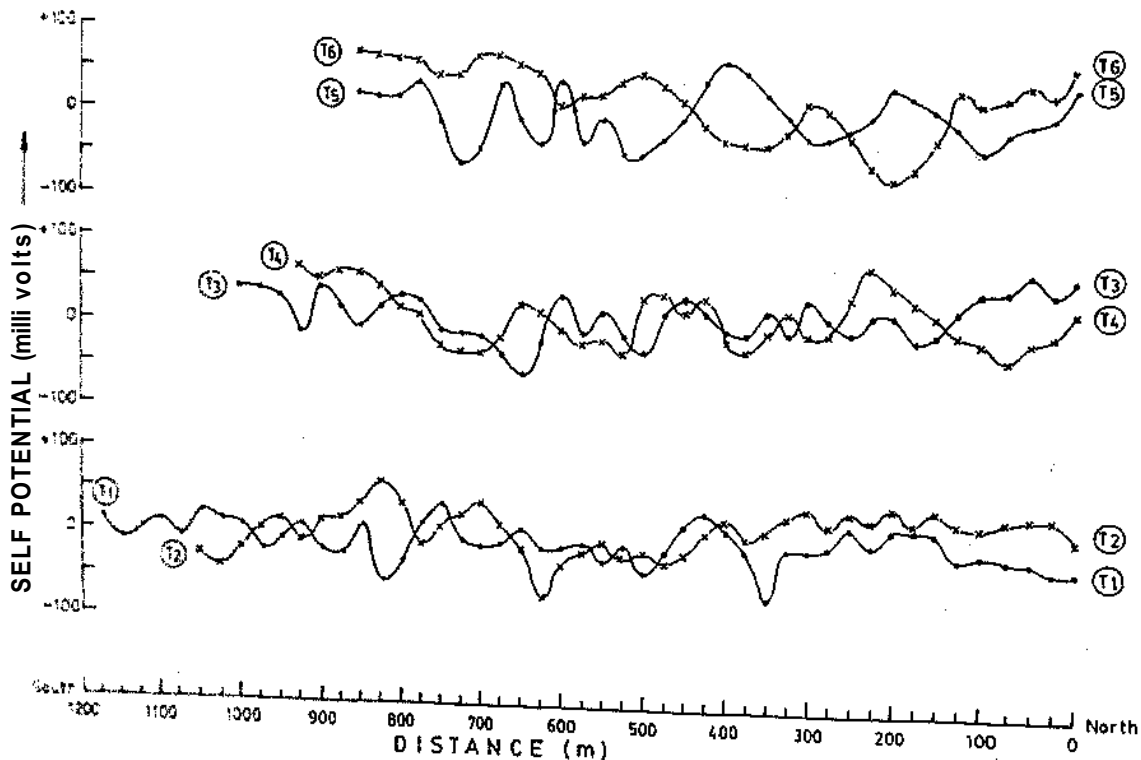


Fig. 10. Self-potential profiles in Schirmacher Oasis.

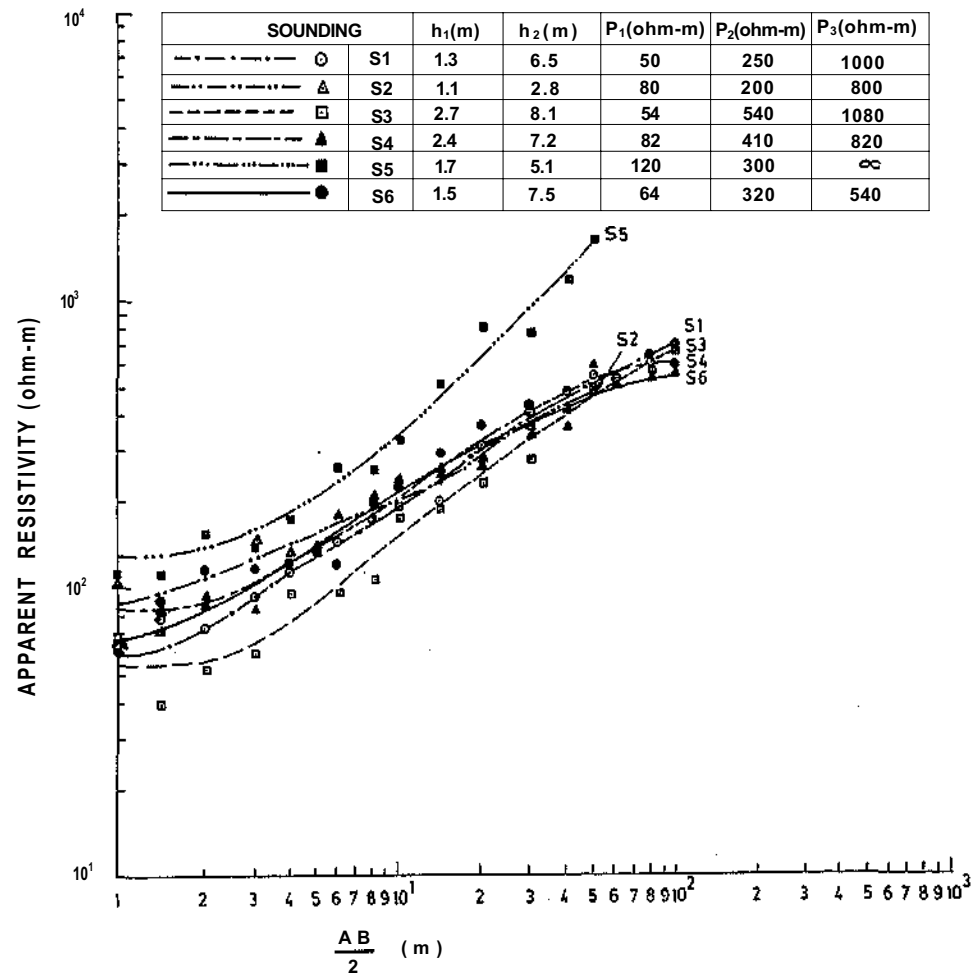


Fig. 11. VES curves in Schirmacher Oasis.

bases. Six VES soundings (S1 to S6) were also carried out over the oasis (Fig. 9). The current electrode separation for the soundings never exceeded 200 m. In addition to these geophysical measurements, four transient electromagnetic (TEM) soundings (1 to 4) were carried out over the ice covered areas. Excepting one station to the south of the oasis (2), all the other TEM sounding stations were on the shelf ice. An approximate square loop size of 50m X 50m to 500m X 500m were used. At each sounding point, more than two loop sizes have also been used.

The self-potential survey does not show any anomaly. The profiles are featureless showing the local noise pattern and some of these are shown in Fig. 10. Fig. 11 shows a few VES sounding curves. The curves are mostly three layers curves of A-type and in all the cases fresh rock in the oasis is very shallow, i.e., less than 10 m. The intermediate layer is 3 to 8 m thick glacial moraine underlying the top soil cover of 1 to 2 m thickness.

All the transient field response was obtained in the form of $e(t)/I$ and the measurements were carried out for 1 to 9 channels each at intervals of 1 m-sec. The theoretical response obtained in the earlier section (equation 7) is for the loop in the air. It is equally valid for any finite conducting medium overlain by thick ice. The response curves thus obtained theoretically have been used for matching with the field curves.

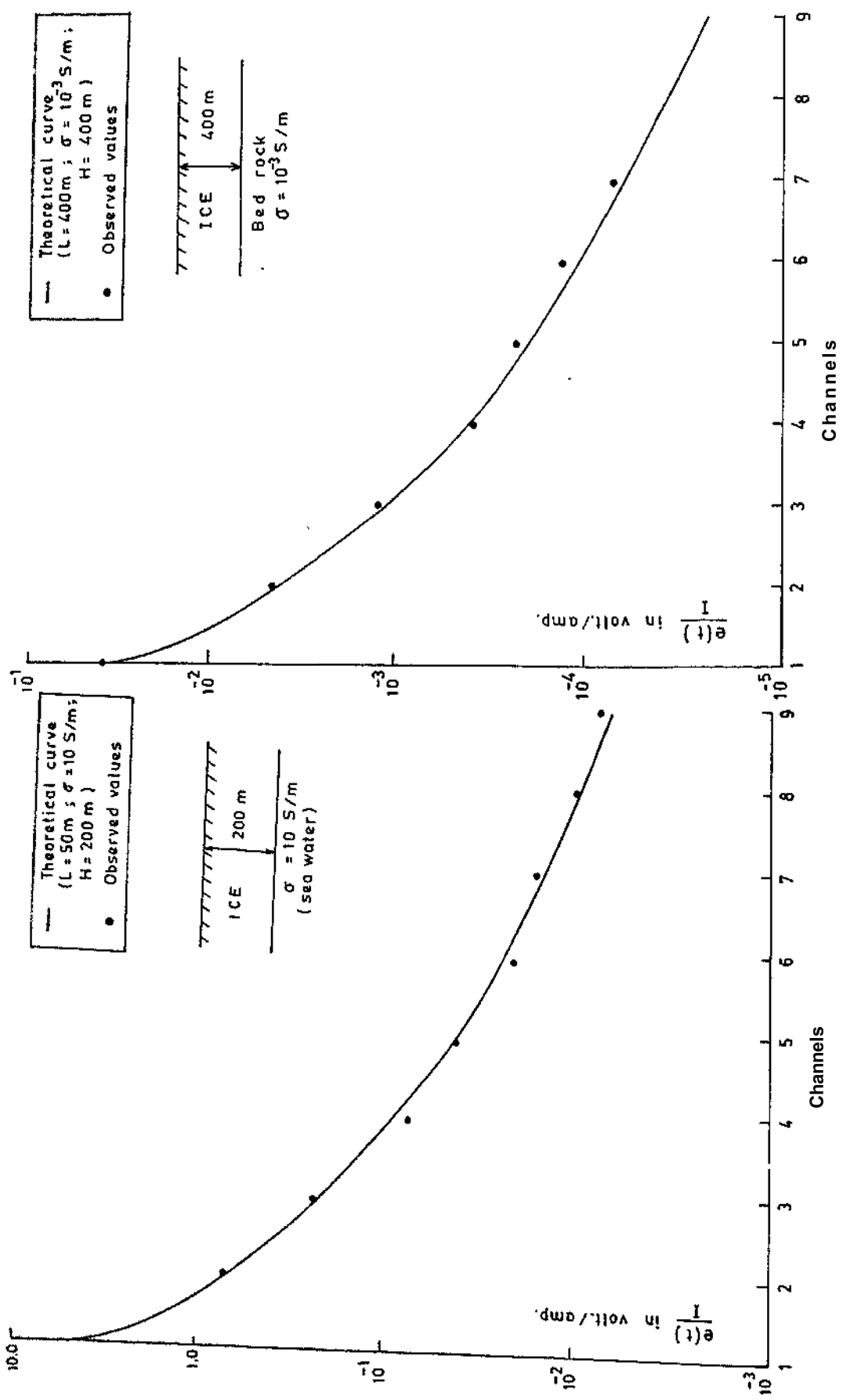


Fig. 12. Field and theoretical TEM curves over the shelfice.

Fig. 13. Field and theoretical TEM curves on an ice cap covering the rocky surface, south of Schirmacher Oasis.

Three TEM soundings (1, 3, 4) were made in the shelf area and only one (2) on the ice cap south of the Schirmacher Oasis (Fig. 8). The loop sizes in the shelf area varied from 50m X 50m to 200m X 200m and for the other (2), it varied from 200m X 200m to 500m x 500 m. The observed data were matched with the album of the theoretical curves already prepared on the basis of the equation (7). Two field results for the sounding points 1 (Fig. 12) and 2 (Fig. 13) are shown here. The results obtained for 1, 3 and 4 are practically the same. Fig. 12 shows that the thickness of the ice shelf to be equal to 200 m. The conductivity of the sea water below the ice shelf has been considered as 10 S/m. Fig. 13, on the other hand, shows that the thickness of the ice cap as 400 m. The resistivity of the underlying metamorphic rocks below the ice cap has been assumed to be equal to 1000 ohm-m as VES curves (S1 to S6) show that the resistivity of the fresh metamorphic rock in this area is about 100 ohm-m.

The thickness of the ice shelf is fairly in good agreement with the results obtained by the Soviet seismic team near Lazarev coast (Atlas Antarktiki, Vol. 1,1966), about 40 km northeast of Dakshin Gangotri station (Fig. 8). The thickness of the ice cap south of the Schirmacher Oasis, however, remains unchecked in the absence of data from any other source including drilling.

CONCLUSIONS

Transient electromagnetic method is quite useful in measuring the thickness of the ice cap including the shelf area. Reconnaissance self-potential measurements are featureless. However, a reliable self-potential interpretation is possible only after a detailed SP map is available for the oasis. Thickness of the glacial morain in the oasis varies from 3-8 m and the hard rock is within a depth of 10 m.

ACKNOWLEDGEMENTS

The author is thankful to his colleagues, specially Cap. K.L. Gajria and Maj. R.K. Tripathi for their assistance in the field work.

REFERENCES

- Atlas Antarktiki, Vol. 1,1966. Glavnoe Upravlenie Geodezii i Karlografi MG USSR, Moscow, 225 (in Russian).
- Bhattacharya, I.S. and R.S. Raju, 1986. *Multifrequency electromagnetic prospecting unit*, R & D Project Report of ISM, 65 pp.
- Gradshteyn, I.S. and I.M. Ryzhik, 1965. *Table of Academic Press, New York, 1086 pp.*
- Kaul, M.K., S.K. Chakraborty and V.K. Raina 1985. Geology of the Dakshin Gangotri Landmass, Schirmacher Hill, Antarctica. *Scientific Report of Second Indian Expedition to Antarctica*, Technical Publication No. 2, Department of Ocean Development, New Delhi, p. 1-10.
- Morrison, H.P., R.J. Phillips and D.P. O'Brien, 1969. Quantitative interpretation of transient electromagnetic fields over a layered half-space. *Geophysical Prospecting*, 17: 82-101.
- Olav, Orhein, 1978. Glaciological studies by Landsat imagery of perimeter of Dronning Maud Land, Antarctica. *Results from Norwegian Antarctic Research 1974-77*, Norsk Polar Institute, p. 69-80.
- Raina, V.K., M.K. Kaul and S.K. Chakraborty, 1985. Ice shelf studies at and around Indian Scientific Research Station, Dakshin Gangotri, Antarctica. *Scientific Report of Second Indian Expedition to Antarctica*, Technical Publication No. 2, Department of Ocean Development, New Delhi, p. 75-80.
- Raju, R.S., M. Keramat and B.B. Bhattacharya, 1987. Design and development of MPPPO transient electromagnetic system and its interpretation techniques for homogenous earth. *Diamond Jubilee Monograph of Department of Applied Geophysics, ISM, Oxford & IBH Publishers Ltd., Calcutta (in press).*
- Sengupta, Sudipta, 1986. Geology of Schirmacher range (Dakshin Gangotri), East Antarctica. *Scientific Report of Third Indian Expedition to Antarctica*, Technical Publication No.3, Department of Ocean Development, New Delhi, p. 187-217.
- Sing, R.K., 1986. Geology of Dakshin Gangotri Hill Range, Antarctica. *Scientific Report of Third Indian Expedition to Antarctica*, Technical Publication No. 3, Department of Ocean Development, New Delhi, p. 181-185.